Perturbation theory of solid-liquid interfacial free energies of bcc metals

Vadim B. Warshavsky and Xueyu Song
Ames Laboratory and Department of Chemistry, Iowa State University, Ames, Iowa 50011, USA
(Received 26 June 2012; published 18 September 2012)

A perturbation theory is used to calculate bcc solid-liquid interfacial free energies of metallic systems with embedded-atom model potentials. As a reference system for bcc crystals we used a single-occupancy cell, hard-sphere bcc system. Good agreements between the perturbation theory results and the corresponding results from simulations are found. The strategy to extract hard-sphere bcc solid-liquid interfacial free energies may have broader applications for other crystal lattices.

DOI: 10.1103/PhysRevE.86.031602 PACS number(s): 68.08.−p, 64.10.+h

I. INTRODUCTION

In our previous study [1] we developed a perturbative approach to calculate solid-liquid interfacial (SLI) free energies and applied it to model systems with inverse power potentials, Lennard-Jones potential and embedded-atom models (EAMs) of metallic systems. In all the considered cases involving fcc crystals we have found reasonable agreements with the corresponding results from molecular simulations. In the present paper we apply the method of Ref. [1] to calculate bcc solid-liquid interfacial free energies of EAM metallic systems.

Essential inputs to the perturbation theory are the thermodynamical and structural properties of a reference system. When an fcc crystal system is studied, the hard-sphere (HS) fcc crystal is commonly chosen as a reference system. These properties of a HS fcc crystal were extensively investigated using molecular simulations [2], density functional theories (DFTs) [3], cell and free volume theories [4,5]. Reliable information is available for free energies [6,7], density distributions [8,9], equations of state [10], and correlation functions [11] in a wide range of densities, from metastable states to close-packing ones.

Unlike the HS fcc crystal, it is problematic to obtain the thermodynamical and structural properties of a HS bcc crystal by conventional molecular simulations due to the mechanical instability of a HS bcc crystal. At the same time, studies of a HS bcc crystal also failed using other theoretical methods. For instance, many DFT studies [12–15] provide unphysical behaviors for a HS bcc crystal, and the free volume method does not provide reliable free energies for a HS bcc solid [16] either.

So far the only way to stabilize a HS bcc crystal in simulations is to enforce some constraints on the center of hard spheres, for example, the location of a HS center is restricted by the bcc Wigner-Seitz cell [17], namely, the single-occupancy cell (SOC) model [6]. It is known that the SOC model provides essentially the same results as the unconstrained simulations for several fcc crystal model systems such as HS, Lennard-Jones potential, and inverse power potentials [18–21]. Therefore it will be interesting to study whether the SOC model of a HS bcc crystal can provide a reliable reference system given the failure of other theoretical methods. In addition, molecular simulations for the SOC HS bcc system are available in literature. For example, in Refs. [16,21] the dependence of pressure on the bulk density is calculated using molecular dynamics simulations (MDSs), and in Ref. [12] the free energy and Gaussian parameters of density distributions are found for two bulk densities using Monte Carlo simulations (MCSs).

Since crystal-orientation-dependent HS bcc solid-liquid interfacial free energies $\gamma_{\rm bcc}^{\rm (HS)}$ are crucial input parameters to our perturbation theory for interfacial free energies of other systems, a strategy to obtain these inputs is essential. Unlike the case for HS fcc solid-liquid $\gamma_{\rm fcc}^{\rm (HS)}$, which is well documented in literature (see, for instance, Refs. [22,23]) using various simulation methods, only a few indirect estimations of $\gamma_{\rm bcc}^{\rm (HS)}$ are available [24,25] using different theoretical methods which involved various approximations. In our study we extract the $\gamma_{\rm bcc}^{\rm (HS)}$ from the bcc solid-liquid interfacial free energies $\gamma_{\rm bcc}^{\rm (SS)}$ of soft-sphere systems, which were obtained from molecular simulations in Ref. [22]. The success of this strategy may open a door for the extraction of solid-liquid free energies involving different crystal lattices.

The rest of the paper is organized as follows: The perturbation theory for the solid-liquid interfacial free energies is briefly reviewed and the input information used in the perturbation theory are presented in Sec. II. The main results of this report are presented in Sec. III. Some concluding remarks are given in Sec. IV.

II. THEORETICAL DEVELOPMENT

In this section we briefly review the perturbation theory for bulk solid and liquid Helmholtz free energy [26,27] and for solid-liquid interfacial free energies [1] so that the input information to the perturbation theory can be presented in a self-contained fashion. Consider a molecular system with interaction potential $\psi(r)$. Let the potential $\psi(r)$ be separated into a short-ranged, purely repulsive reference part $\psi_{\rm ref}(r)$ and a perturbative part $\psi_{\rm pert}(r)$. For a system with an interaction potential which is purely repulsive $\psi(r) \sim 1/r^n$, the parameter of separation λ is chosen simply as $\lambda = R_1$ [13,28], where R_1 is a nearest-neighbor distance (for bcc lattice $R_1 = \frac{3^{1/3}}{2^{2/3}\rho^{1/3}}$ and ρ the bulk density). The reference system is then mapped onto an effective HS system with a temperature-dependent HS diameter $d(T)$ prescribed by Weeks-Chandler-Anderson (WCA) criterion [26,27,29]. The resulting expression for the total Helmholtz free energy is

$$F = F_{hs} + F_{\rm pert}, \tag{1}$$

where F_{hs} is the HS free energy, $F_{\rm pert}$ the perturbative part of the free energy [30,31]:

$$F_{\rm pert} = \frac{1}{2}\rho \int d\vec{r}\, g_{hs}(r/d)\psi_{\rm pert}(r). \quad (2)$$

In the above equations g_{hs} is the averaged correlation function of the HS reference system [31–33].

Recently we have developed a perturbation approach to calculate the solid-liquid interfacial free energies [1], thus extending the perturbation approach to interfacial properties. In the framework of this approach the interfacial free energy γ is expressed as

$$\gamma = \gamma_{hs} + \gamma_{\rm pert}, \quad (3)$$

where γ_{hs} is the interfacial free energy of a reference HS system. The perturbative part $\gamma_{\rm pert}$ can be written as

$$\gamma_{\rm pert} = \sum_{i=1}^{3} \left\{ \frac{F_\alpha^i}{A} - \frac{1}{2}\left(f_\alpha^s \rho^s + f_\alpha^l \rho^l\right)\Delta z_{hs} \right\}, \quad (4)$$

where

$$F_1^{(i)} = \frac{1}{2}\iint d\vec{r}_1 d\vec{r}_2 \rho(\vec{r}_1)\rho(\vec{r}_2) g_{hs}(\vec{r}_1,\vec{r}_2)\psi_{\rm pert}(\vec{r}_1,\vec{r}_2), \quad (5)$$

$$F_2^{(i)} = k_B T \int d\vec{r}\, \rho(\vec{r}) \log[\rho(\vec{r})/\rho_{hs}(\vec{r})], \quad (6)$$

$$F_3^{(i)} = -\frac{k_B T}{2}\int d\vec{r}_1 d\vec{r}_2 c_{hs}^{(2)}(\vec{r}_1,\vec{r}_2)[\rho(\vec{r}_1) - \rho_{hs}(\vec{r}_1)] \times [\rho(\vec{r}_2) - \rho_{hs}(\vec{r}_2)]. \quad (7)$$

In the above expression, $\rho(\vec{r})$ is the density profile of the interfacial region, $g_{hs}(\vec{r}_1,\vec{r}_2)$ the correlation function, $c_{hs}(\vec{r}_1,\vec{r}_2)$ the direct correlation function, and $\rho_{hs}(\vec{r})$ the density profile of the HS interfacial region. ρ^s and ρ^l are the coexisting bulk solid and liquid densities, f^s and f^l the Helmholtz free energy per particle in coexisting solid and liquid phases, Δz_{hs} the width of the HS reference interfacial region, A the area of the interface, k_B the Boltzmann constant, and T the temperature. For the embedded-atom model (EAM) of metals, suitable generalizations of Eqs. (1) and (3) can be made for the case of many-body EAM potentials [1,34,35], and more details of the calculations can be found in Ref. [1].

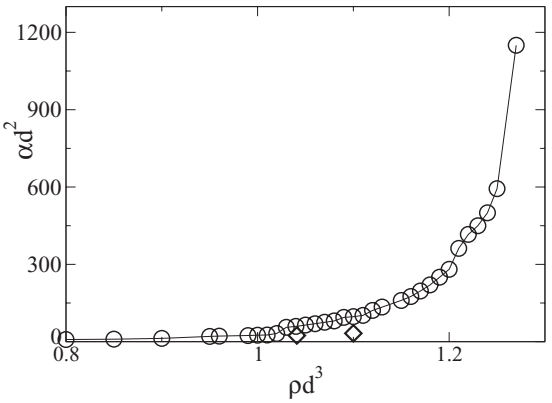

FIG. 1. Dimensionless parameters of Gaussian distribution αd^2 vs density ρd^3 for the SOC HS bcc system. Results are obtained from Monte Carlo simulations (MCSs). The circles are from our simulations and the diamonds are from Ref. [12]. The line is only a guide to the eye.

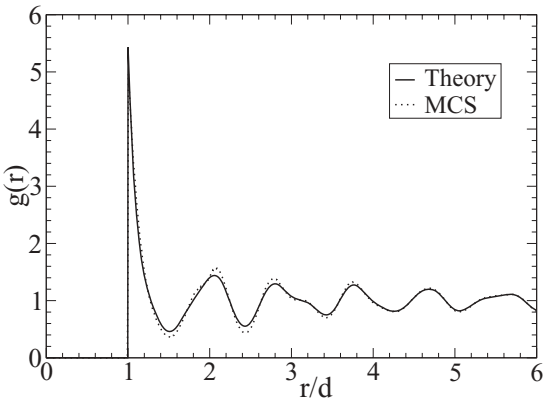

FIG. 2. A representative correlation function $g(r)$ of the SOC HS bcc system for $\rho d^3 = 1.0$. The bold line is the result obtained from the theory of Rascon *et al.* [32] (Theory) and the dotted line is the result from our Monte Carlo simulations (MCSs).

For a HS SOC bcc crystal, the dependence of pressure on density could be found in Ref. [21]. The Helmholtz free energy can be calculated, using a thermodynamic integration, from the data of Ref. [21]. For the Gaussian parameter α of a one-body density distribution in this reference system, Monte Carlo simulations of the SOC model are performed and the result is shown in Fig. 1. Our simulations yield the same equation of state as in Ref. [21], and the Gaussian parameter is close to the ones in Ref. [12] at the same reduced densities.

If free energies of a HS SOC bcc system f^s and the Gaussian parameters α are known, the method of Rascon *et al.* [32] can be implemented to calculate the correlation functions $g_{hs}^s(r/d)$. In Fig. 2 a typical correlation function $g_{hs}^s(r/d)$ obtained from the theory of Ref. [32] as well the one from our Monte Carlo simulations at density $\rho d^3 = 1.0$ is shown to agree with each other. Hence the theory of Ref. [32] for correlation functions can be used not only for the constrained HS crystals, but also for SOC HS systems.

III. RESULTS

To test the validity of the SOC HS bcc reference system, we have calculated the bcc solid-liquid coexistence conditions for soft-sphere systems with the inverse power potential $\psi(r) = \epsilon(\sigma/r)^n$, where $n = 6$, 7, and 8. The coexistence conditions are obtained from the double-tangent Maxwell construction

TABLE I. Bcc solid-liquid coexistence conditions (n is a parameter of the inverse power potential, ρ_s^*, ρ_l^*, and P^* the dimensionless solid and liquid densities and pressure). Results of the perturbation theory (PT) are compared with the ones from molecular dynamics simulations (MDSs) [22].

	PT			MDS		
n	ρ_s^*	ρ_l^*	P^*	ρ_s^*	ρ_l^*	P^*
6	2.370	2.281	97.70	2.326	2.299	100.0
7	1.890	1.812	61.09	1.861	1.834	63.88
8	1.621	1.549	43.85	1.607	1.578	47.1

TABLE II. Crystal-orientation-dependent HS bcc solid-liquid interfacial free energies $\gamma_{100}^{(HS)}$, $\gamma_{110}^{(HS)}$, $\gamma_{111}^{(HS)}$ for $n = 6,7,8$ of inverse power potentials (see explanation in text). Units of γ are $\beta\gamma d^2$.

n	$\gamma_{100}^{(HS)}$	$\gamma_{110}^{(HS)}$	$\gamma_{111}^{(HS)}$
6	0.416	0.399	0.406
7	0.411	0.390	0.401
8	0.407	0.388	0.397
av	0.411	0.392	0.402

using the liquid and solid free energies βf ($\beta = 1/k_BT$) as a function of $1/\rho$. Table I shows the calculated coexisting bcc solid $\rho_s^* = \rho_s\sigma'^3$ and liquid $\rho_l^* = \rho_l\sigma'^3$ densities and pressure $P^* = \beta P\sigma'^3$, where $\sigma' = (\beta\epsilon)^{1/n}\sigma$, and the corresponding results from molecular simulations [22]. Good agreements between the results of the perturbation theory and simulations demonstrated the validity of the SOC HS bcc crystal as a reference system.

To apply our perturbation theory to interfacial free energies γ involving a bcc crystal with various interaction potentials, the reference HS bcc interfacial free energies $\gamma_{bcc}^{(HS)}$ are essential. As a direct simulation between a HS bcc crystal and liquid interface is not possible, we adopt an indirect strategy to extract the HS interfacial free energies involving a SOC bcc crystal. In our previous work we have demonstrated that the perturbation theory for interfacial free energies is accurate for various fcc systems [1] and accurate bcc-liquid interfacial free energies of inverse-power potentials are known from simulations [22]. A combination of our perturbation theory and the bcc-liquid interfacial free energies of the inverse power potentials from simulations can be used to calculate the SOC HS bcc-liquid interfacial free energies, namely,

$$\gamma^{(HS)} = \gamma^{(SS)} - \gamma_{pert}, \tag{8}$$

where $\gamma^{(SS)}$ is the interfacial free energies from MD simulations [22], and γ_{pert} can be calculated from our perturbation theory [Eq. (4)].

The results for $\gamma^{(HS)}$ are listed in Table II. It is seen that for a given crystal orientation for $n = 6,7,8$ of the inverse power potential $\gamma^{(HS)}$ values are slightly different, which may reflect inherent errors of the perturbation theory (for $n > 8$ the bcc HS crystal becomes metastable and hence simulation results are not available [22]). The averaged values represent our best estimate for $\gamma^{(HS)}$ and are shown in the last row of Table II. Our results are $\gamma_{100}^{(HS)} = 0.411$, $\gamma_{110}^{(HS)} = 0.392$, and $\gamma_{111}^{(HS)} = 0.402$. Previously, HS bcc solid-liquid interfacial free energies have been estimated in Ref. [25] ($\gamma_{bcc} = 0.43$) and Ref. [24] ($\gamma_{bcc} = 0.47$) using different theoretical methodologies. Our result represents the first reliable estimate for HS bcc solid-liquid interfacial free energies at different crystal orientations and can be used to predict the bcc solid-liquid interfacial free energies of any interaction potentials.

As an example, we have calculated the bcc solid-liquid interfacial free energies of several EAM metallic systems where simulation or experimental results exist. Two different EAM potentials for Fe, the ABCH [36] and the MH(SA)^2 model [37], and the EAM potential for Zr [38], are studied in the present report. As the perturbation calculations are done under zero pressure, the melting temperature T_m can be determined by the crossing point of solid and liquid free energy curves as a function of temperature T for each EAM system [34]. The potential separation parameter λ was chosen to be $\lambda = (R_1 + R_2)/2$, where R_2 is the next-to-nearest neighbors distance [for bcc lattice $R_2 = (2/\rho)^{1/3}$]. The results for coexisting solid ρ_s and liquid ρ_l densities as well as for melting temperature T_m, enthalpy of fusion $l_m = h_l - h_s$, and Turnbull's constant $c_T = \gamma_0/(l_m\rho_s^{2/3})$ are presented in Table III and are compared with the ones from simulations [38,39]. Agreements between the results of present perturbation theory and simulations are found to be similar to other systems involving different crystal lattices [35]. For example, the difference in T_m for Fe(ABCH) is 3.0%, for Fe[MH(SA)^2] is -9.2%, for Zr is 4.5%. The enthalpy per particle h is calculated using a thermodynamic formula

$$h = \frac{F}{N} - T\frac{\partial\left(\frac{F}{N}\right)}{\partial T} - \frac{P}{\rho}. \tag{9}$$

[If the dependence of F_{EAM} and F_{pert} on temperature T is weak, then the following equation is valid: $h = \frac{3}{2}k_BT + \frac{F_{EAM}}{N} + \frac{F_{pert}}{N} + \frac{P}{\rho}$. For the metal systems under consideration, we have found that the enthalpy h obtained from this equation is not very accurate as compared to the one obtained from Eq. (9).]

TABLE III. Calculated melting temperature T_m, coexisting solid ρ_s and liquid ρ_l densities, enthalpy of fusion l_m, Turnbull's coefficient c_T, average SLI free energies γ_0, and the anisotropy parameters ϵ_1 and ϵ_2 for various EAM potentials. Results of the perturbation theory (PT) are compared with the ones from MDS (Ref. [39] for Fe models, Ref. [38] for Zr coexistence) and experiments (EXPT) (Ref. [40] for Zr SLI free energies).

	PT			MDS/EXPT		
	Fe(ABCH)	Fe[MH(SA)^2]	Zr	Fe(ABCH)	Fe[MH(SA)^2]	Zr
T_m (K)	2430.5	1608.3	2203.4	2358.7	1772.0	2109
ρ_s (Å^{-3})	0.0770	0.0799	0.0410	0.0784	0.0801	0.0411
ρ_l (Å^{-3})	0.0746	0.0763	0.0407	0.0737	0.0763	0.0408
l_m (eV/atom)	0.111	0.074	0.084	0.218	0.162	0.179
c_T	0.55	0.69	0.77	0.32	0.36	–
γ_0 (mJ/m^2)	176.2	152.1	123.2	206	175	115
ϵ_1 (%)	9.05	5.08	6.37	1.6	3.3	–
ϵ_2 (%)	2.32	1.77	2.01	− 0.04	0.24	–

Finally, we computed bcc solid-liquid interfacial free energies of the EAM metallic systems using the perturbation theory. The calculated average interfacial free energy γ_0 and anisotropy parameters ϵ_1 and ϵ_2 at zero pressure are given in Table III (for definitions of γ_0, ϵ_1, and ϵ_2, see, for instance, Ref. [1]). The results are compared to the ones from simulations [39] for Fe models and to experimental measurements for Zr of Ref. [40]. (There is no simulation data for bcc solid-liquid interfacial free energies with the EAM Zr potential [38] available in literature.) Again, results for the obtained average bcc SLI free energies γ_0 are in satisfactory agreement with results from simulations or experiments. For example, for Fe(ABCH) the error is 14.5%, Fe(MHSA$_2$) 13.0%, and Zr 7.0%.

IV. CONCLUDING REMARKS

In Ref. [1] we have developed a perturbative method for theoretical calculations of fcc crystal and melt interfacial free energies. Good agreements between the theoretical results and the results from simulations are found for all the considered EAM metal systems. In addition, we have demonstrated the possibility to extract liquid-crystal interfacial free energies for fcc hard-sphere systems. In the present study we extended this method to bcc solid-liquid systems of EAM metals. As it is well known that the HS bcc crystal is unstable with respect to shear deformations and conventional simulation methods cannot be used to calculate the thermodynamic properties of the HS bcc system, at the same time various theoretical approaches to the HS bcc system also failed [12–15]. In this report we demonstrated that a single-occupancy cell model of the HS bcc system can be used as a reference system. In combination with the thermodynamic properties of the HS bcc system from literature [21] and Gaussian parameters α of the one-body density distribution as a function of density from our Monte Carlo simulations, we were able to extend the perturbation theory to various systems involving bcc crystals. More importantly, such a strategy can be used for any crystal lattices of HS systems. The obtained bcc solid-liquid coexistence conditions for inverse power potentials are in good agreement with the results from molecular simulations (Table I). The HS bcc solid-liquid interfacial free energies $\gamma_{\rm bcc}^{\rm (HS)}$ are extracted from a combination of simulation results [22] and our perturbation theory, and hence provide the first reliable estimates for these quantities. The obtained $\gamma_{\rm bcc}^{\rm (HS)}$ is in good agreement with a previous estimation of Ref. [25]. Since our calculations are based upon a perturbation approach, our coexistence conditions agree with the simulation results reasonably well; hence we will expect that the relative stabilities between the bcc and fcc phases are similar to the simulation results, which is well documented for inverse power potentials [41].

As further applications of our methodology, Fe and Zr solid-liquid coexistence conditions and interfacial free energies with EAM potentials are studied. The results for melting temperatures as well as for bcc interfacial free energies are again in reasonable agreement with the ones from simulations and experiments (Table III).

We have used the fundamental measure density functional theory (FM DFT) [42,43] to calculate thermodynamic and structural properties of the SOC HS bcc system and found similar unphysical results as in Ref. [14]. Therefore, the current fundamental measure functionals are not suitable for the calculations of a SOC HS bcc reference system. The reason for the excises is that FM DFT can be directly generalized to multicomponent mixtures, thus providing the thermodynamic and structural information of binary or ternary SOC HS bcc systems much more efficiently than simulations. The latter can be used as reference systems for a perturbation theory to study bcc binary alloys, just as the perturbation theory for fcc binary alloys which was previously developed in Ref. [35]. So far, discovery of a useful functional for a HS bcc crystal remains a challenge.

ACKNOWLEDGMENTS

This research was sponsored by the Division of Materials Sciences and Engineering, Office of Basic Energy Sciences, US Department of Energy, under Contract No. W-7405-ENG-82 with Iowa State University (V.B.W. and X.S.) and by NSF Grant No. CHE-0809431(XS).

[1] V. B. Warshavsky and X. Song, J. Phys.: Condens. Matter **22**, 364112 (2010).
[2] D. Frenkel and B. Smit, *Understanding Molecular Simulation: From Algorithm to Application*, 2nd ed. (Elsevier, New York, 2002).
[3] R. Evans, in *Fundamentals of Inhomogeneous Fluid,* edited by D. Henderson (Wiley, New York, 1992).
[4] A. Munster, *Statistical Thermodynamics* (Springer-Verlag, Berlin, 1974), Vol. II.
[5] J. A. Barker, J. Chem. Phys. **63**, 632 (1975).
[6] W. G. Hoover and F. H. Ree, J. Chem. Phys. **49**, 3609 (1968).
[7] D. Frenkel and A. J. C. Ladd, J. Chem. Phys. **81**, 3188 (1984).
[8] D. A. Young and B. J. Alder, J. Chem. Phys. **60**, 1254 (1974).
[9] R. Ohnesorge, H. Lowen, and H. Wagner, Europhys. Lett. **22**, 245 (1998).
[10] K. R. Hall, J. Chem. Phys. **57**, 2252 (1972).
[11] Y. Choi, T. Ree, and F. H. Ree, J. Chem. Phys. **95**, 7548 (1991).
[12] W. A. Curtin and K. Runge, Phys. Rev. A **35**, 4755 (1987).
[13] J. F. Lutsko and M. Baus, Phys. Rev. A **41**, 6647 (1990).
[14] J. F. Lutsko, Phys. Rev. E **74**, 021121 (2006).
[15] E. Velasco, L. Mederos, and G. Navascues, Mol. Phys. **97**, 1273 (1999).
[16] S. K. Kwak, T. Park, Y. Yoon, and J. Lee, Mol. Simul. **38**, 16 (2012).
[17] N. W. Ashcroft and N. D. Mermin, *Solid State Physics* (Saunders College, Philadelphia, 1976).
[18] J-P. Hansen and L. Verlet, Phys. Rev. **184**, 151 (1969).

[19] J-P. Hansen, Phys. Rev. A **2**, 221 (1970).
[20] W. G. Hoover, M. Ross, K. W. Johnson, D. Henderson, J. A. Barker, and E. C. Brown, J. Chem. Phys. **52**, 4931 (1970).
[21] L. V. Woodcock, Faraday Discuss. **106**, 325 (1997).
[22] R. L. Davidchack and B. B. Laird, Phys. Rev. Lett. **94**, 086102 (2005).
[23] Y. Mu, A. Houk, and X. Song, J. Phys. Chem. **109**, 6500 (2005).
[24] D. W. Marr and A. Gast, J. Chem. Phys. **99**, 2024 (1993).
[25] L. Granasy and T. Pusztai, J. Chem. Phys. **117**, 10121 (2002).
[26] J. D. Weeks, D. Chandler, and H. C. Andersen, J. Chem. Phys. **54**, 5237 (1971).
[27] H. S. Kang, T. Ree, and F. H. Ree, J. Chem. Phys. **84**, 4547 (1986).
[28] H. S. Kang, C. S. Lee, T. Ree, and F. H. Ree, J. Chem. Phys. **82**, 414 (1985).
[29] L. Verlet and J. Weis, Phys. Rev. A **5**, 939 (1972).
[30] J. Hansen and I. McDonald, *Theory of Simple Liquids*, 2nd ed. (Academic Press, San Diego, CA, 1986).
[31] C. Rascon, L. Mederos, and G. Navascues, Phys. Rev. Lett. **77**, 2249 (1996).
[32] C. Rascon, L. Mederos, and G. Navascues, Phys. Rev. E **54**, 1261 (1996).
[33] C. Rascon, L. Mederos, and G. Navascues, J. Chem. Phys. **105**, 10527 (1996).
[34] X. Song and J. R. Morris, Phys. Rev. B **67**, 092203 (2003).
[35] V. B. Warshavsky and X. Song, Phys. Rev. B **79**, 014101 (2009).
[36] G. J. Ackland, D. J. Bacon, A. F. Calder, and T. Harry, Philos. Mag. A **75**, 713 (1997).
[37] M. I. Mendelev, S. Han, D. J. Srolovitz, G. J. Ackland, D. Y. Sun, and M. Asta, Philos. Mag. **83**, 3977 (2003).
[38] M. I. Mendelev and G. J. Ackland, Philos. Mag. Lett. **87**, 349 (2007).
[39] D. Y. Sun, M. Asta, and J. J. Hoyt, Phys. Rev. B **69**, 174103 (2004).
[40] M. J. Wert, W. H. Hofmeister, and R. J. Bayuzick, J. Appl. Phys. **93**, 3643 (2003).
[41] R. Agrawal and D. A. Kofke, Mol. Phys. **85**, 23 (1995).
[42] R. Roth, R. Evans, A. Lang, and G. Kahl, J. Phys.: Condens. Matter **14**, 12063 (2002).
[43] P. Tarazona, Physica A **306**, 243 (2002).